Spherical shell model description of rotational motion

A. P. Zuker,[1] J. Retamosa,[2] A. Poves,[2] and E. Caurier[1]

[1]*Physique Théorique, Bâtiment 40/1 CRN, Institut National de Physique Nucléaire et des Particles-CNRS/Université Louis Pasteur, Boîte Postale 28, F-67037 Strasbourg Cedex 2, France*

[2]*Departamento de Física Teórica, Universidad Autónoma de Madrid, E-28049 Madrid, Spain*

Exact diagonalizations with a realistic interaction show that configurations with four neutrons in a major shell and four protons in another—or the same—major shell, behave systematically as backbending rotors. The dominance of the $q \cdot q$ component of the interaction is related to an approximate "quasi-SU3" symmetry. It is suggested that the onset of rotational motion in the rare earth nuclei is due to the promotion of the eight particle blocks to the major shells above the ones currently filling. Assuming a "pseudo-SU3" coupling for the particles in the lower orbits, it is possible to account remarkably well for the observed $B(E2)$ rates at the beginning of the region.

PACS number(s): 21.60.Cs, 21.60.Ev, 21.60.Fw

The SU(3) model of Elliott [1] provides a microscopic description of rotors that exhibit spectra in $J(J+1)$. For sufficiently low J, or sufficiently large representations they became perfect in the sense of having a constant intrinsic quadrupole moment $Q_0 = Q_0(J)$, where

$$Q_0(J) = \frac{(J+1)(2J+3)}{3K^2 - J(J+1)} \langle JJ|3z^2 - r^2|JJ \rangle, \qquad (1)$$

as postulated in the strong coupling limit of the unified model of Bohr and Mottelson [2].

Since the quadrupole force that appears in the SU(3) Casimir operator is also an important part of the nuclear interaction [3,4], we expect it to play a determinant role in the onset of rotational motion in real nuclei—the problem we want to address. A direct approach would demand, in general, diagonalizations in spaces of two major shells in neutrons and protons as first proposed by Kumar and Baranger [5]. Dimensionalities are then of order 10^{40}, exceeding by far what is possible at present (10^7) [6].

Therefore, it is necessary to develop a computational strategy, and our starting point will consist in learning as much as we can from situations in which neutrons and protons are independently restricted to a single major shell, that can be the same close to $N = Z$: Exact calculations will show that rotational features, including the systematic appearance of backbending, are determined by the interplay of the quadrupole force with the central field, in the subspace of a major shell spanned by the sequence of $\Delta j = 2$ orbits that comes lowest under the spin-orbit splitting. This state of affairs will be explained by the existence of an approximate symmetry (quasi-SU3), which when combined with pseudo-SU3 provides the coupling scheme capable of explaining the onset of rotational motion. We use the following notations: ν=neutrons, π=protons, $C^{lm} = \sqrt{4\pi/(2l+1)}Y^{lm}$, $q \equiv q^{2m} = r^2 C^{2m}$. p is the principal quantum number, r_p is the generic label for all orbits in the pth oscillator shell *except* the largest (i.e., $j = j_{max} = p + 1/2$). We use l for $j = l + 1/2$ orbits in the sense $h = h_{11/2}$, $g = g_{9/2}$, $p = p_{3/2}$, etc., except in the

following convention: pfh means the full $p = 5$ shell, i.e., $p_{1/2}, p_{3/2}, f_{5/2}, f_{7/2}, h_{9/2}, h_{11/2}$, while $hfp = h_{11/2} f_{7/2} p_{3/2}$, and similarly for other shells.

Although a space of a full major shell, with very specific single-particle spacings, is necessary to ensure strict SU(3) symmetry, we know of several examples where the ds or fp subspaces produce rotorlike spectra in the presence of spin-orbit splittings: $(ds)^4$ describes ^{20}Ne quite well [7] and $(ds)_\pi^{3,4}(fp)_\nu^2$ configurations explain the onset of deformation in ^{31}Na and ^{32}Mg [8]. Furthermore ^{48}Cr provides the first example of a backbending band in $N = Z$ nuclei. The experimental spectrum [9] is almost perfectly reproduced by a full $(pf)^8$ shell model calculation, with strong indications that the $(fp)^8$ space is sufficient to explain the quadrupole coherence [10]. The situation has a double interest. As we shall see later, configurations that consist of four protons in a major shell and four neutrons in another (the same in $N \approx Z$) play a key role in the onset of rotational motion in heavier nuclei, and the restriction to the $\Delta j = 2$ spaces makes the diagonalizations possible, as illustrated by the four cases we are going to treat (in parenthesis the corresponding m-scheme dimensionalities):

$$(fp)^8 T_z = 0; (2 \times 10^4), \quad (fp)_\pi^4 (gds)_\nu^4; (1.1 \times 10^5),$$

$$(gds)^8 T_z = 0; (6 \times 10^5), \quad (gds)_\pi^4 (hfp)_\nu^4; (1.9 \times 10^6),$$

against

$$(pf)^8 T_z = 0; (2 \times 10^6), \quad (pf)_\pi^4 (sdg)_\nu^4; (10^7),$$

$$(sdg)^8 T_z = 0; (5 \times 10^7), \quad (sdg)_\pi^4 (pfh)_\nu^4; (1.9 \times 10^8).$$

We shall compare the results obtained with the KLS interaction [11] and with pure quadrupole forces using $\hbar \omega = 9$ MeV with a uniform single-particle spacing $\varepsilon = 1$ MeV, corresponding to the standard $-\beta \ell \cdot s$ splitting ($\beta \approx 20 A^{-2/3}$ MeV and $\hbar \omega \approx 40 A^{-1/3}$) [12].

It has been shown in [4] that for one shell the quadrupole component of a general realistic interaction has the form $-e_2 \bar{q}_p \cdot \bar{q}_p$, where e_2 goes as $A^{-1/3}$ and, $\bar{q}_p = q_p / \mathcal{N}_p^{(2)}$ is the
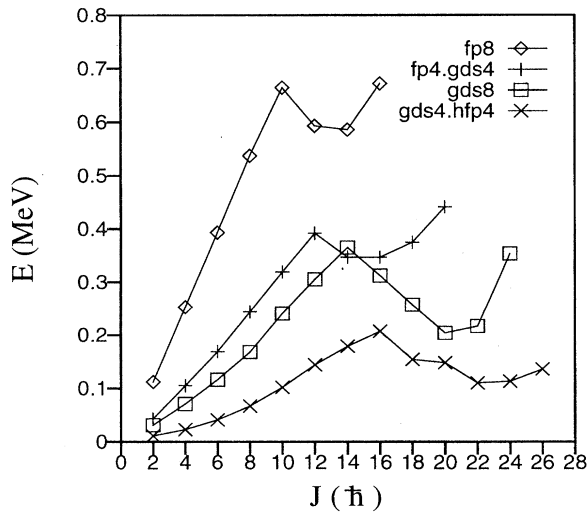
FIG. 1. Yrast transition energies $E_\gamma = E(J+2) - E(J)$ for different configurations, KLS interaction.

FIG. 2. Yrast transition energies $E_\gamma = E(J+2) - E(J)$ for the $(gds)^8$ configuration with an $-e_2\bar{q}\cdot\bar{q}$ force.

quadrupole operator q_p in shell p, normalized by $\mathcal{N}_p^{(2)}$—the square root of the sum of the squares of the matrix elements of q_p—which goes as $(p+3/2)^2$. For two contiguous shells the force is $-e_2(\bar{q}_p + \bar{q}_{p+1})\cdot(\bar{q}_p + \bar{q}_{p+1})$, with the same e_2 coupling, and it differs markedly from the traditional $\chi(q_p + q_{p+1})\cdot(q_p + q_{p+1})$, with $\chi = O(A^{-5/3})$ [3].

Figure 1 shows the yrast bands in the four spaces. Rotational behavior is fair to excellent at low J. As expected from the normalization property of the realistic quadrupole force the moments of inertia in the rotational region go as $(p+3/2)^2$ $(p'+3/2)^2$, i.e., if we multiply all the E_γ values by this factor the lines become parallel. The Q_0 values are constant to within 5% up to a critical J value at which the bands backbend.

Since all the spaces behave in the same way we specialize to $(gds)^8$ in what follows. Figure 2 shows the results of diagonalizing $e_2 \bar{q}_p \cdot \bar{q}_p$ $(p=4)$. At $e_2 = 9.6$ the ε splittings are overwhelmed and we have a nearly perfect rotor. The value of Q_0 stays practically constant up to $J = 16$–18 and then decreases slowly. At $e_2 = 4.8$, 3.2, and 2.4 the rotational behavior remains very good below $J = 14$. Then there is a break and the upper values are again aligned. At $e_2 = 3.2$ the overlap of each state with the one obtained with the full KLS interaction is always better than $(0.95)^2$, which suggests that

$$\langle h | \mathscr{H} | h \rangle_J \approx \langle q | \mathscr{H} | q \rangle_J,$$

where $|h\rangle$ and $|q\rangle$ are the eigenstates of the full Hamiltonian $\mathscr{H}$ and the quadrupole force $(e_2 = 3.2)$, respectively. Figure 3 shows that this is the case indeed. It means that the observed backbending pattern is obtained by doing first-order perturbation theory on $|q\rangle$: the spectrum changes but not the structure (i.e., the wave functions). A similar situation is found when comparing the full $(pf)^8$ calculation with a renormalized interaction and $\varepsilon = 2$ (Fig. 10 of Ref. [10]) and the $(fp)^8$ result in Fig. 1: the backbend occurs at the same J and the Q_0 values are very close in spite of a much larger
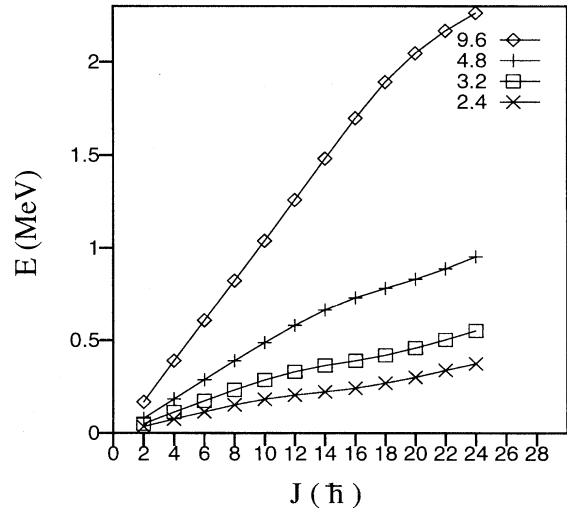
slope (i.e., smaller moment of inertia) in the bigger calculation. Here again, the variation in moment of inertia is a perturbative effect [13].

To gain some insight into the backbending phenomenon we examine the evolution of the wave functions and quadrupole moments. In Fig. 4 we find that for $e_2 = 9.6$ the percentage of the g^8 configuration in the full eigenstate is very small and nicely correlated with the Q_0 values. This is what we expect from a good rotor, for which the amplitudes of any configuration (not only g^8) must be J independent (since all states must be projections of the same intrinsic state). For the KLS results and their $e_2 = 3.2$ counterparts $Q_0(J)$ decreases abruptly above $J = 14$, while the g^8 configuration increases its amplitude and becomes dominant in the region where $Q_0(J)$ reaches a plateau. It is clear that at the backbend the notion of intrinsic state loses, or changes, its meaning, and the idea of a band crossing suggested by Fig. 2 becomes
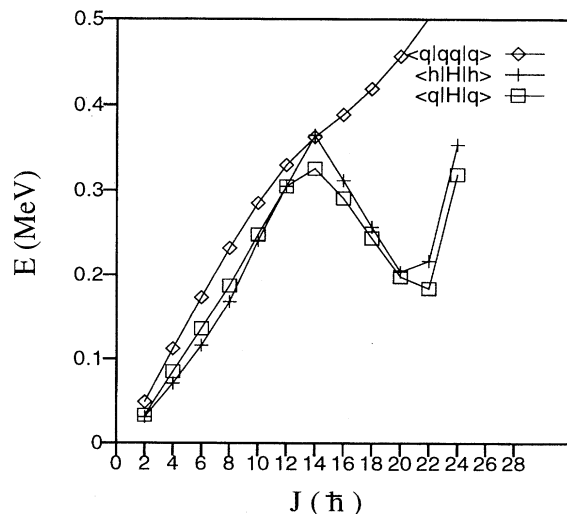

FIG. 3. $\langle h | \mathscr{H} | h \rangle = (gds)^8$ in Fig. 3; $\langle q | qq | q \rangle = 3.2$ in Fig. 4 compared with $\langle q | \mathscr{H} | q \rangle$. See text.
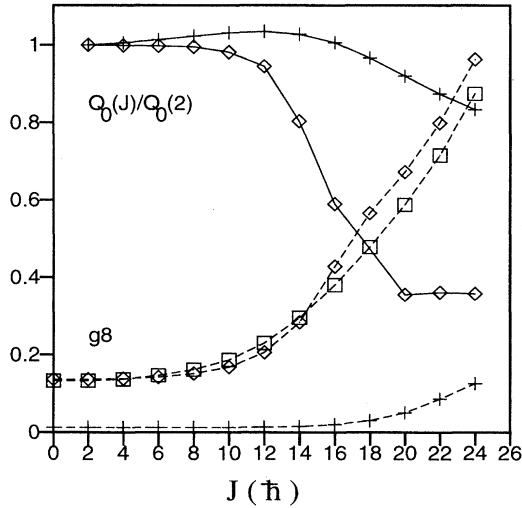
FIG. 4. $Q_0(J)/Q_0(2)$ (full lines) and $g_8 = \langle g^8|(gds)^8\rangle^2$ (dashed lines). Wave functions calculated with $-e_2\bar{q}\cdot\bar{q}$ (crosses $\equiv e_2 = 9.6$, squares $\equiv e_2 = 3.2$) and KLS (diamonds).

FIG. 5. Nilsson orbits for SU(3) $(k=2p)$ and quasi-SU3 $(k=2p-1/2)$.

questionable. The connection of our results with those of cranked mean-field calculations [14] is explored in a forth-coming publication [13].

That the build up of quadrupole coherence needs only the lower $\Delta j = 2$ sequence of the full shell can be understood by examining Table I where we list the matrix elements of $q^{20} = r^2 C^{20} = \frac{1}{2}(3z^2 - r^2)$, in jj and LS coupling. It is seen that the $\Delta j = 1$ matrix elements are small, both for m small (prolate shapes) and m large (oblate). If we simply neglect them, diagonalizing the $\Delta j = 2$ matrix in jj scheme is very much equivalent to diagonalizing the exact q^{20} operator in LS scheme. This amounts to saying that the sequence $j = 1/2, 5/2, 9/2, \ldots$ (or $j = 3/2, 7/2, 11/2, \ldots$) must behave very much as an $l = 0, 2, 4, \ldots$ (or $l = 1, 3, 5, \ldots$) one. Therefore we introduce a new operator (the "quasi" q^{20}), defined in the $\Delta j = 2$ space via the following replacements in the LS matrix elements of q^{20}: $l \rightarrow j$, $p \rightarrow p + 1/2$, $m \rightarrow m + 1/2$ and $-m \rightarrow -m - 1/2$: $(m > 0)$.

In Fig. 5 we draw to the left the spectrum of the full q^{20} operator (in fact $2q^{20}$), i.e., the SU(3) Nilsson orbits. The bandheads come at $2(p + 3/4 - 3/2|m|)$. To the right we have plotted the spectrum of the "quasi" $2q^{20}$ operator. Now the bandheads are at $2(p + 1/2 - 3/2|m|)$, that is, the exact LS values, except for $m = \pm 1/2$, where the one to one corre-
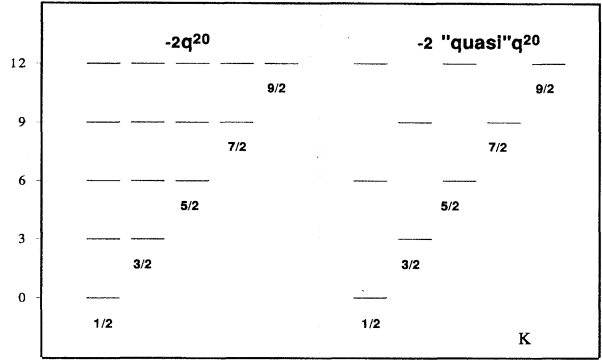
spondence between the "quasi" q^{20} and the exact q^{20} in LS scheme breaks down. The corresponding "quasi-SU3" symmetry cannot be exact because of this (small, $<1\%$) mismatch. The spectrum of the true q^{20} operator in the $\Delta j = 2$ space is extremely close to the one in Fig. 5, and it is clear that the amount of quadrupole coherence obtained by filling the m (or K) = 1/2 and 3/2 orbits is almost as large as for the SU(3) orbitals. For the eight particle blocks we are interested in, the intrinsic Q_0 would be

$$Q_0 = 8[e_\pi(p_\pi - 1) + e_\nu(p_\nu - 1)]. \qquad (2)$$

The Q_0 values obtained with the $q \cdot q$ interaction at $e_2 = 9.6$ saturate the value predicted by Eq. (2) within 2% while at $e_2 = 2.4$ we still have 80% of this limit.

It is interesting to note that in an SU(3) scheme, the two possible fillings in Fig. 5 for four particles lead to nonaxially symmetric rotors. For quasi-SU3, the filling is unique and we expect therefore axial symmetry, which in the absence of an observed γ band, seems to be the case in ^{48}Cr.

The indications obtained so far are of use in suggesting a computational strategy for more general situations.

It is only exceptional, as in ^{20}Ne or ^{48}Cr, that ground-state rotational bands involve only one major shell. Usually, two are needed, and to fix ideas we examine how we would go about a shell model calculation in the space shown in Fig. 6 [3]. For the lower shells the sequence of orbits is the conventional one, and for the upper (empty) ones we have assumed a spin-orbit splitting, which may be naive, but it is correct in the light nuclei and consistent with the (scarce)

TABLE I. The matrix elements of r^2 and C_{20} in jj and LS coupling.

$\langle pl|r^2|pl\rangle = p + 3/2$

$\langle jm|C_2|jm\rangle = \dfrac{j(j+1) - 3m^2}{2j(2j+2)}$

$\langle jm|C_2|j+1m\rangle = -\dfrac{3m[(j+1)^2 - m^2]^{1/2}}{(2j+4)(2j+2)(2j)}$

$\langle jm|C_2|j+2m\rangle = \dfrac{3}{2}\left\{\dfrac{[(j+2)^2 - m^2][(j+1)^2 - m^2]}{(2j+2)^2(2j+4)^2}\right\}^{1/2}$

$\langle pl|r^2|pl+2\rangle = -[(p-l)(p+l+3)]^{1/2}$

$\langle lm|C_2|lm\rangle = \dfrac{l(l+1) - 3m^2}{(2l+3)(2l-1)}$

$\langle lm|C_2|l+2m\rangle = \dfrac{3}{2}\left\{\dfrac{[(l+2)^2 - m^2][(l+1)^2 - m^2]}{(2l+5)(2l+3)^2(2l+1)}\right\}^{1/2}$
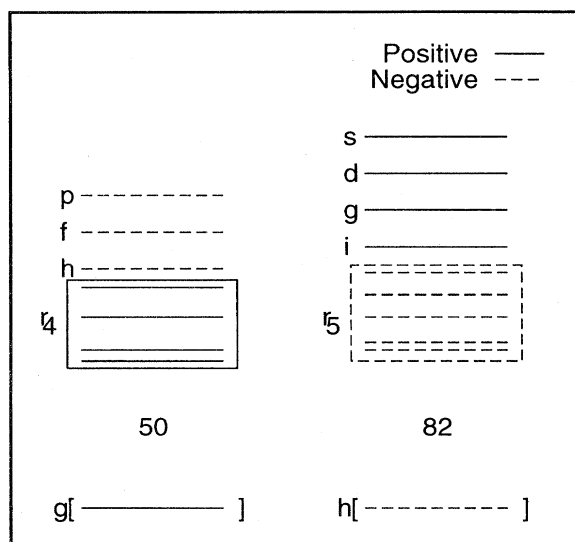
FIG. 6. Schematic single-particle spectrum above ^{132}Sn.

available data in the heavier ones. *Mutatis-mutandis*, the same scheme applies to the $Z=28$, $N=50$ and $Z=82$, $N=126$ closures.

We do not aim directly at exact solutions, but at sufficiently good ones to do perturbation theory on them. Therefore, according to what we learned in Fig. 3, it should be sufficient to diagonalize the quadrupole force in the presence of the single particle, or more generally, monopole field [15,16]. Then, the number of particles in *each* of the four major shells in Fig. 6 is a good quantum number. Now, start by assuming the quadrupole force to be so strong that SU(3) becomes an exact symmetry. Since each representation is closed under the quadrupole operator, the problem of finding eigenstates would be reduced to one of coupling different representations. In other words, the basis in each block (major shell) would consist of a small number of states for each J. Naturally, the most interesting would be those associated with the lowest representations, obtained by filling the lowest orbits in the left of Fig. 5. The general idea is that the breakdown of SU(3) will be such that the exact symmetry may be replaced by an approximate one, so that the calculations could proceed under similar lines. It is clear that quadrupole dominance will lead to enormous computational gains, and

TABLE II. $B(E2)\uparrow$ in e^2b^2 compared with experiment [21].

N	Nd	Sm	Gd	Dy
92	4.47	4.51	4.55	4.58
	2.6(7)	4.36(5)	4.64(5)	4.66(5)
94	4.68	4.72	4.76	4.80
			5.02(5)	5.06(4)
96	4.90	4.95	4.99	5.03
			5.25(6)	5.28(15)
98	5.13	5.18	5.22	5.26
				5.60(5)

what follows provides a clue on the viability of the approach we have outlined.

Granted that quasi-SU3 operates in the upper shells in Fig. 6, we need a counterpart for the lower ones. Since the r_p groups in the figure are pseudo-oscillator shells, the pseudo-SU3 symmetry of Arima, Draayer, Harvey, and Hecht is an excellent candidate (Ref. [17] contains a recent survey). The situation is seen to be quite analogous to the one for exact SU(3), but now the most interesting states are obtained by filling the lowest orbits to the left and right of Fig. 5 for the lower and upper shells, respectively. The quasi-SU3 symmetry can be more than an interpretative tool, as made clear by the constancy of Q_0 and its closeness to the theoretical maximum given by Eq. (2) even with relatively weak quadrupole couplings. If we assume that the same is true for pseudo-SU3, we may estimate Q_0 for some typical rare earth rotors.

The number of particles in each shell for which the energy will be lowest will depend on a balance of monopole and quadrupole effects, but we can tentatively borrow from Nilsson diagrams [18,19] a result common to different regions and to different calculations: When nuclei acquire stable deformation, two orbits $K=1/2$ and $3/2$, originating in the upper shells of Fig. 6, become occupied. In spherical terms it means that the upper group is an 8-particle configuration $(hfp)^4_\pi(igds)^4_\nu$, of the type we have studied. Following this hint, a very rough treatment of the monopole-quadrupole balance is capable of detecting the onset of deformation and of providing ground-state binding energies with an rms error of some 250 keV [20]. Let us take then Q_0 for the upper shell from Eq. (2) with $p_\pi=5$, $p_\nu=6$, and consider even-even nuclei with $Z=60$–66 and $N=92$–98, corresponding to 6 to 10 protons with pseudo-$p=3$, and 6 to 10 neutrons with pseudo-$p=4$ in the lower shells. From the left part of Fig. 5 we obtain easily their contribution to Q_0, which added to that of Eq. (2) yields a total

$$Q_0 = 56e_\pi + (76 + 4n)e_\nu, \qquad (3)$$

for $^{152+2n}$Nd, $^{154+2n}$Sm, $^{156+2n}$Gd, and $^{158+2n}$Dy, respectively. Note that, at fixed n, the value is constant in the four cases because the orbits of the triplet $K=1/2$, $3/2$, $5/2$ in Fig. 5 have zero contribution for $p=3$. Q_0 (given in dimensionless oscillator coordinates, i.e., $r \rightarrow r/b$ with $b^2 \approx 1.01A^{-1/3}$ fm^2), is related to the $E2$ transition probability from the ground state by $B(E2)\uparrow = 10^{-5}A^{2/3}Q_0^2$. The results, using effective charges of $e_\pi=1.4$, $e_\nu=0.6$ calculated in [4] are compared in Table II with the available experimental values [21]. The agreement is quite remarkable especially if we consider that no parameters enter the calculation. (It is interesting to note that the "regional" systematics of [22] call upon formulas similar to Eq. (3), but need much larger effective charges.) The discrepancy in Table II in ^{152}Nd is likely to be of experimental origin, since systematics indicate, with no exception, much larger rates for a 2^+ state at such low energy (72.6 keV).

The assumption that the upper blocks consist of eight particles has been checked by considering possible alternatives and the only one that cannot be ruled out easily involves $6\nu4\pi$ promotion. However, energetically it is not favored

because the very slight gain in quadrupole coherence could hardly compensate the monopole loss. Furthermore, it would entail low lying γ bands in places where they are not seen. In all other cases the agreement deteriorates, not only in the magnitudes but in the trends along the isotopic and isotonic lines. It is worth noting that for 16 particles in the upper shells the $B(E2)$ can reach a value of $8e^2b^2$. However this is probably an underestimate, because by then, the effective couplings between the blocks may increase sufficiently to push the systems into yet other variants of SU(3), or even the exact symmetry.

The famous low lying $4p$-$4h$ states in ^{16}O and ^{40}Ca are early examples of the general mechanism we are proposing for rotational nuclei. In the next oscillator closure, at ^{80}Zr [23], the intruders become ground states. From then on $8p$-$8h$

excitations seem necessary to ensure the observed quadrupole coherence, and something akin to rotor-rotor coupling operates between major shell blocks. It appears that the spherical description of rotational motion rests on variants of the SU(3) symmetry, which may supplement, and eventually extend, the standard mean field theories. In particular the tendency of quadrupole forces of Elliott type to produce clustering in the excited states [24,25] will probably lead to significant differences of interpretation between the spherical and deformed formulations for large quadrupole moments.

[1] J. P. Elliott, Proc. R. Soc. London **245**, 128,562 (1956).
[2] A. Bohr and B. Mottelson, Math. Fis. Medd. Dan. Vid. Selsk **27**, No. 161 (1953).
[3] M. Baranger and K. Kumar, Nucl. Phys. **A110**, 490 (1968).
[4] M. Dufour and A. P. Zuker, Report No. nucl-th9505010, submitted to Phys. Rev. C.
[5] K. Kumar and M. Baranger, Nucl. Phys. **A110**, 529 (1968).
[6] ANTOINE code, CRN, Strasbourg, 1989 (to be released).
[7] A. Arima, S. Cohen, R. D. Lawson, and M. McFarlane, Nucl. Phys. **A108**, 94 (1968).
[8] A. Poves and J. Retamosa, Nucl. Phys. **A571**, 221 (1994).
[9] J. A. Cameron, *et al.*, Phys. Lett. B **319**, 58 (1993).
[10] E. Caurier, A. P. Zuker, A. Poves, and G. Martínez-Pinedo, Phys. Rev. C **50**, 225 (1994).
[11] S. Kahana, H. C. Lee, and C. K. Scott, Phys. Rev. **180**, 956 (1969); **185**, 1378 (1969).
[12] A. Bohr and B. Mottelson, *Nuclear Structure* (Benjamin, New York, 1964), Vol. 1.
[13] E. Caurier, J. L. Egido, G. Martínez, A. Poves, J. Retamosa, L. M. Robledo, and A. P. Zuker, Phys. Rev. Lett. (in press).
[14] J. L. Egido and L. M. Robledo, Phys. Rev. Lett. **70**, 2876 (1993).
[15] A. P. Zuker and M. Dufour, Report No. nucl-th9505012, submitted to Phys. Rev. C.
[16] A. P. Zuker, Nucl. Phys. **A576**, 65 (1994).
[17] J. P. Draayer, in *Future Directions in Nuclear Physics with $4\pi\gamma$ Detection Systems of the New Generation*, edited by J. Dudek and B. Haas, AIP Conf. Proc. No. 259 (AIP, New York, 1992).
[18] S. G. Nilsson, Mat. Fys. Medd. Dan. Vid. Selsk. **29**, 1 (1955).
[19] A. K. Jain, R. K. Sheline, P. C. Wood, and K. Jain, Rev. Mod. Phys. **62**, 393 (1990).
[20] J. Duflo and A. P. Zuker, Phys. Rev. C **52**, R1 (1995).
[21] S. Raman, C. W. Nestor, S. Kahane, and K. H. Bhatt, At. Data Nucl. Data Tables **42**, 1 (1989).
[22] S. Raman, C. W. Nestor, and K. H. Bhatt, Phys. Rev. C **37**, 805 (1988).
[23] C. J. Lister *et al.*, Phys. Rev. Lett. **69**, 1270 (1987).
[24] D. M. Brink, in *Course XXXVI Enrico Fermi School*, edited by C. Bloch (Academic, New York, 1966).
[25] Y. Abgrall, G. Baron, E. Caurier, and G. Monsonego, Phys. Lett. **24B**, 609 (1967); **26B**, 53 (1967).